Journal of Plant Interactions

ISSN: 1742-9145 (Print) 1742-9153 (Online) Journal homepage: https://www.tandfonline.com/loi/tjpi20

Biosynthesis of artemisinin – revisited

Nishi Srivastava & Anand Akhila

To cite this article: Nishi Srivastava & Anand Akhila (2011) Biosynthesis of artemisinin – revisited, Journal of Plant Interactions, 6:4, 265-273, DOI: 10.1080/17429145.2011.570869

To link to this article: https://doi.org/10.1080/17429145.2011.570869

Journal of Plant Interactions
Vol. 6, No. 4, December 2011, 265–273

Taylor & Francis
Taylor & Francis Group

ORIGINAL ARTICLE

Biosynthesis of artemisinin – revisited

Nishi Srivastava and Anand Akhila*

Department of Chemistry, Central Institute of Medicinal and Aromatic Plants, Lucknow 226 015, India

(Received 28 December 2010; final version received 8 March 2011)

Artemisinin is a well-known antimalarial drug isolated from the *Artemisia annua* plant. The biosynthesis of this well-known molecule has been reinvestigated by using [1-^{13}C]acetate, [2-^{13}C]acetate, and [1,6-$^{13}C_2$]glucose. The ^{13}C peak enrichment in artemisinin was observed in six and nine carbon atoms from [1-^{13}C]acetate and [2-^{13}C]acetate, respectively. The ^{13}C NMR spectra of ^{13}C-enriched artemisinin suggested that the mevalonic acid (MVA) pathway is the predominant route to biosynthesis of this sesquiterpene. On the other hand, the peak enrichment of five carbons of ^{13}C-artemisinin including carbon atoms originating from methyls of dimethylallyl group of geranyl pyrophosphate (GPP) and farnesyl pyrophosphate (FPP) was observed from [1,6-$^{13}C_2$]glucose. This suggested that GPP which is supposed to be biosynthesized in plastids travels from plastids to cytosol through the plastidial wall and combines with isopentenyl pyrophosphate (IPP) to form the (*E*,*E*)-FPP which finally cyclizes and oxidizes to artemisinin. In this way the DXP pathway also contributes to the biosynthesis of this sesquiterpene.

Keywords: *Artemisia annua*; artemisinin; biosynthesis; sesquiterpene; ^{13}C-NMR; mevalonic acid pathway (MVA); deoxyxylulose pyrophosphate pathway (DXP)

Introduction

Artemisinin (**21**) is a sesquiterpene lactone bearing an endoperoxide ring. This is a unique feature found in this sesquiterpene and also considered to be responsible for the effective treatment of malaria caused by the multidrug-resistant *Plasmodium falciparum* (Liu et al. 1979; WHO 1981; Klayman et al. 1984; Klayman 1985). It is derived from the glandular secretory trichomes present in the leaves and flowers of the *Artemisia annua* plant. The increasing trends of malaria throughout the world and the resistance of existing drugs have increased the demand of this naturally occurring sesquiterpene. Researchers are putting maximum effort for the last 25 years to obtain large amounts of artemisinin through synthesis or by enhancing the yields in the plant through biotechnological methods (Delabays et al. 2001; Sy and Brown 2002; Ferreira et al. 2005; Ro et al. 2006; Putalun et al. 2007). In order to achieve higher targets through in vivo and in vitro systems, the knowledge of biosynthetic pathway from the earliest precursors to artemisinin is essential. A lot of publications have come up over the last 25 years giving information on the biosynthesis of artemisinin (**21**) (Akhila et al. 1987; Schramek et al. 2010) artemisinic acid (**14**) (Akhila et al. 1990; Covello et al. 2007), and amorphadiene (Bouwmeester et al. 1999) by using ^{14}C and ^{13}C-labeled precursors.

The complete pathway to artemisinin can be divided into three steps: (1) biosynthesis of farnesyl pyrophosphate (FPP, **9**) from CO_2, acetate, glucose, and isopentenylpyrophosphate (IPP, **6**)/dimethylallylpyrophosphate (DMAPP, **7**) (C_5 units) through the mevalonic acid (MVA) or non-MVA pathways; (2) cyclization of FPP (**9**) to amorphadiene (**13**); and (3) biosynthesis of artemisinic acid (**14**), dihydroartemisinic acid (**15**), and artemisinin (**21**) from amorphadiene (**13**). The biosynthesis of artemisinic acid (**14**) (Akhila et al. 1990) and artemisinin (**21**) (Akhila et al. 1987) was studied using ^{14}C and ^{3}H-labeled precursors in which the biosynthetic intermediates were predicted. The mechanism of hydrogen shifts during the cyclization, and oxidations steps were also explored. In one of the reports the mechanism of cyclization of FPP (**9**) by amorpha-4,11-diene synthase (ADS) involving isomerization of FPP (**9**) to (*R*)-nerolidyl diphosphate (NPP, **10**), ionization of NPP (**10**), and C-1,C-6 ring closure to generate a bisabolyl cation, followed by a 1,3-hydride shift, 1,10-ring closure to generate the amorphane skeleton, and deprotonation at either C-12 or C-13 to afford the final product amorphadiene has been discussed (Picaud et al. 2005). ADS uses FPP as substrate, and the isomerization to NPP has been found to occur at the enzyme's active site. The amorphadiene synthase and germacrene A synthase have been isolated and characterized, and this is the most important step in the biosynthesis of isoprenoid compounds and artemisinin in *A. annua*. (Bouwmeester et al. 1999; Mercke et al. 2000; Bertea et al. 2006). ^{13}C and ^{2}H-labeled sesquiterpenes like dihydroartemisinic acid (**15**) and dihydro-epi-deoxyarteannuin have been

*Corresponding author. Email: akhiladr@hotmail.com

ISSN 1742-9145 print/ISSN 1742-9153 online

http://dx.doi.org/10.1080/17429145.2011.570869
http://www.tandfonline.com

used during the last decade to study the biosynthetic mechanism of conversion of artemisinic acid (**14**) to artemisinin (**21**) under in vivo conditions in *A. annua*. (Brown and Sy 2004, 2007a,b).

Recently the focus of research on biosynthesis of artemisinin (**21**) has shifted towards the site of synthesis of intermediate compounds along with artemisinin (**21**) and location of relevant enzymes in different compartments of the cell, ultimately giving information on the existence of MVA or DXP pathways (Olsson et al. 2009). A recent approach in this direction has revealed that artemisinin (**21**) was predominantly biosynthesized from (*E*,*E*) FPP (**9**) whose central isoprenoid unit had been obtained via the non-mevalonate pathway. The isotopologue data confirm the previously proposed mechanism for the cyclization of (*E*,*E*)-FPP to amorphadiene (**13**) and its oxidative conversion to artemisinin (**21**). The experiments were performed on live plants by using an atmosphere of $^{13}CO_2$ (Schramek et al. 2010).

It has been amicably demonstrated now in bacteria and phototrophic eukaryotes that in addition to MVA pathway the DXP path also exists during the formation of IPP (**6**) and DMAPP (**7**) which are the building blocks of all the terpene compounds (Rohmer et al. 1993, 1996; Eisenreich et al. 1997, 1998, 2001; Lichtenthaler 1999; Rohmer 1999; Hoeffler et al. 2002). It has also been established through different piece of works that the mevalonate pathway is responsible for the biosynthesis of sesqui- and triterpenes in the cytoplasm, whereas the DXP pathway operates in plastids for the biosynthesis of mono-, di-, and tetraterpenes along with carotenoids (Arigoni et al. 1997). Thus, both the mechanisms are compartmentalized through the walls of the cell organs. This compartmental separation is not absolute because there have been examples when MVA has been found to be incorporated into monoterpenoidal and diterpenoidal moieties which are supposed to be formed in plastids (Schwarz 1994; Lichtenthaler et al. 1997). There are also reports that both the pathways exist in higher plants, and a 'crosstalk' between the two pathways can be explained by the exchange of metabolic intermediates between the cytoplasm and the plastids (Arigoni et al. 1997; Hemmerlin et al. 2003; Schuhr et al. 2003; Towler and Weathers 2007). In a recent report (Schramek et al. 2010) geranyl pyrophosphate (GPP) (**8**) was shown to cross over the plastidial wall into cytosol and become part of FPP (**9**) which was finally converted to artemisinin (**21**).

In order to re-establish the above facts by using more precise precursors, we decided to conduct the experiments by feeding [1-^{13}C]acetate, [2-^{13}C]acetate, and [1,6-$^{13}C_2$]glucose on live plants of *A. annua*. ^{13}C-labeled precursors have been a useful tool in studying the biosynthetic pathway of terpene compounds. A detailed biogenetic route to IPP and DMAPP through MVA and DXP pathways has been demonstrated by using ^{13}C precursors during the course of studying the biosynthesis of andrographolide (a diterpene) in *Andrographis paniculata* (Srivastava and Akhila 2010).

Materials and methods

Reagents

$CDCl_3$ 1H δ7.24; ^{13}C δ77.0, [1-^{13}C]acetate, [2-^{13}C]acetate, and [1,6-$^{13}C_2$]glucose (>99% isotopic abundance) were purchased from Sigma-Aldrich, USA.

Plant material and feeding methods

Artemisia annua plants grown in the farms of CIMAP were used in this study. Three different methods were tried (Srivastava and Akhila 2010). (1) *Direct-stem injection* – 60-day- old plants (40 cm high, stem: 6 mm wide) were selected, and a needle (0.30 mm) attached with 500 µl syringe (Hamilton) was inserted up to the middle of the stem (about 3 mm) about 20 cm from the flowering tips of the plant. One hundred microliters of 10% solution of ^{13}C-labeled precursor (acetate) was injected over 12 hrs. The feeding of acetate solution was done to 20 sets of plants. All the plant material was pooled and harvested after 15 days and artemisinin (2**1**) was extracted. (2) *Plant cuttings were fed with precursor under normal environmental conditions* – 30- to 40-cm-high plant twigs with intact leaves were grown under non-sterile conditions for about three days in 25 ml Hoagland's medium. The plant cuttings were then transferred to a solution (10 ml in a test tube) of 1% ^{13}C-labeled precursors in separate set of experiments which were supplemented with 2 ml of labeled substrate for 2 weeks and then extracted for desired compound (2**1**). (3) *Precursor uptake by plant cuttings under forced transpiration* – 30- to 40-cm-high plant twigs were maintained on Hoagland's medium for 3 days and then transferred to solution (10 ml in a test tube) of 1% ^{13}C-labeled substrate. This solution was allowed to be taken up by the plant twigs under illumination (a 60 watt bulb) and forced transpiration by an air fan. The uptake of the substrate solution was supplemented by adding ^{13}C-labeled substrate at regular intervals as soon as the level of solution dropped by 2 ml in the test tube holding the plant twigs. After the uptake of desired precursor the twigs were maintained for seven days on sterile medium to avoid contamination. The peak enrichment of desired carbons by direct stem injection method was very poor, showing that the fed-precursor could not enter the site of biosynthesis through a proper path. Similar results were obtained in an earlier experiment also (Srivastava and Akhila 2010). The incorporation of ^{13}C-labeled precursors through stem cuttings under normal conditions was best followed by reasonably good incorporation under forced transpiration uptake of the substrate.

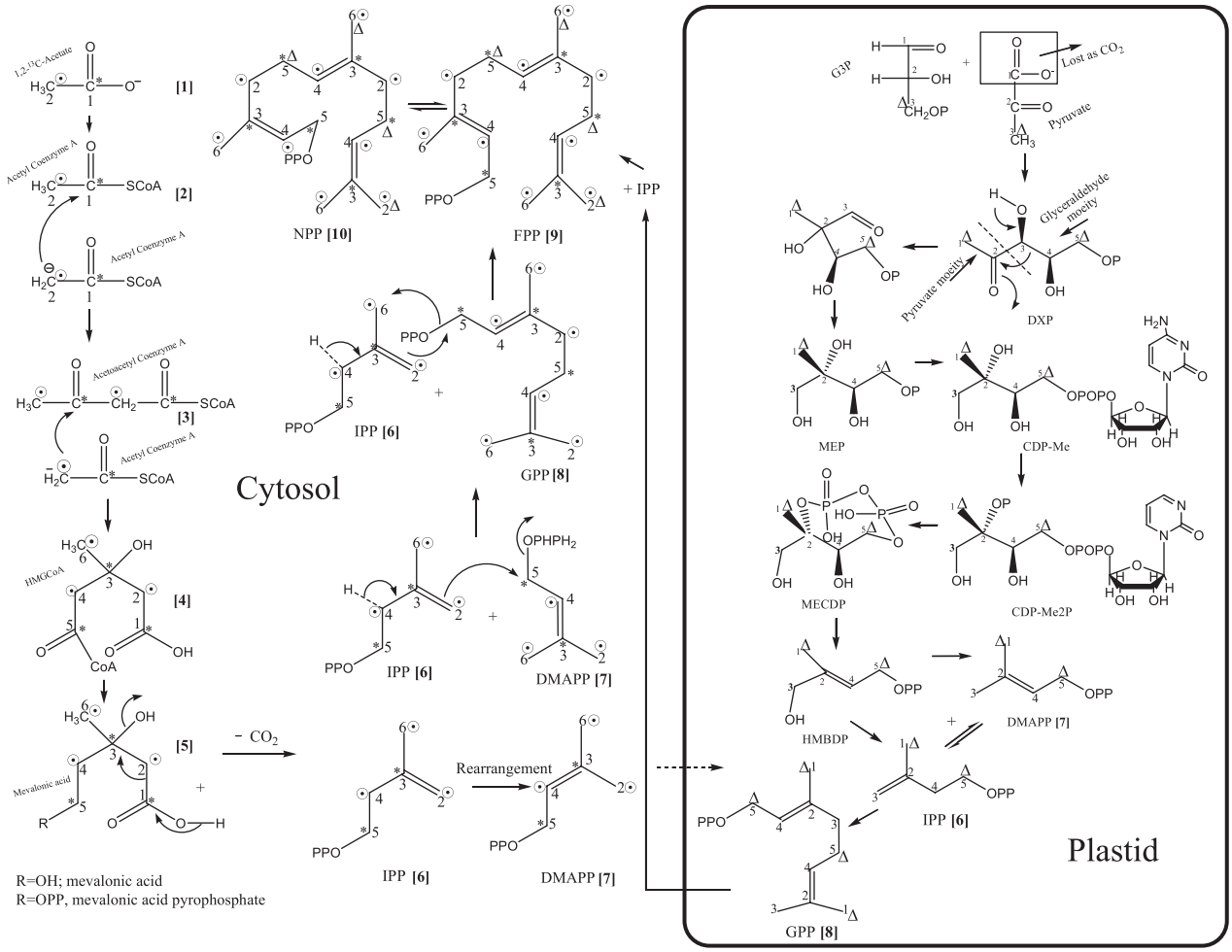

Figure 1. MVA and DXP pathways are shown in cytosol and plastids, respectively. Possibility of C_5 and C_{10} units crossing over the plastidial envelope is shown. *, ⊙, denote label from [1-^{13}C]acetate and [2-^{13}C]acetate, respectively, whereas Δ denotes label from [1,6-$^{13}C_2$]glucose.

Extraction and isolation

The plant twigs (1 kg) which were fed with ^{13}C-labeled precursors in all the above feeding experiments were air-dried, yielding about 200 g of dry plant biomass, and mixed with the dried normal plants (1.8 kg). The pooled herbage (2 kg) was extracted with cold MeOH (3 × 2 l for 24 hrs). The combined extracts were concentrated *in vacuo* to yield 225 g of dark brown residue. The residue was defatted with hexane and then separated by column chromatography (CC) on Si Gel using EtOAc–hexane (as eluent) while increasing the percentage of EtOAc [0:100; 10:90; 20:80; 30:70; 40:60; 50:50; 60:40; 70:30; 80:20] and continuously monitoring the eluted fractions for the presence of **21**. The fractions obtained from EtOAc–hexane (55:50 and 60:40) afforded white crystals of **21** which were again recrystallized from hot MeOH. The structure of **21** was confirmed by ^{1}H and ^{13}C-NMR spectra and its comparison with the spectroscopy data available in the literature (Rimada et al. 2009; Schramek et al. 2010).

Results and discussion

Depending upon the knowledge available in the literature, the ^{13}C-label from C-1(*)-acetate is likely to attain the positions C-1, C-3, and C-5 in MVA (**5**), C-3 and C-5 in IPP (**6**), and DMAPP (**7**). Further, C-1 of MVA is lost during its conversion to IPP (**6**) and DMAPP (**7**), whereas the ^{13}C-label from C-2(⊙) will go to C-2, C-4, and C-6 of IPP (**6**) and DMAPP (**7**) as shown in Figure 1. IPP (**6**) and DMAPP (**7**) are the two building blocks of terpene skeletons, and these are biosynthesized through different mechanisms and routes in cytosol and plastids via MVA and DXP pathways, respectively. Samples of ^{13}C-enriched artemisinin (**21**) were isolated from cold methanol extract of flowering twigs of *A. annua* which were fed with [1-^{13}C]acetate, [2-^{13}C]acetate, and [1,6-$^{13}C_2$]glucose in separate set of experiments. The numbering pattern shown in IPP (**6**), DMAPP (**7**), GPP (**8**), FPP (**9**), and NPP (**10**) adopted in Figure 1 is for the convenience to understand the positions and linkages between the three C_5 units (IPP + DMAPP + IPP). However, the traditional numbering pattern has been adopted in Figures 2 and 3 from numbers 1 to 15 for all the 15 carbons of sesquiterpenes starting from the carbon bearing OPP at C-1. The purified crystals of (**21**) were subjected to ^{13}C-NMR analysis. ^{13}C-enriched artemisinin obtained from [1-^{13}C]acetate showed enhancement of

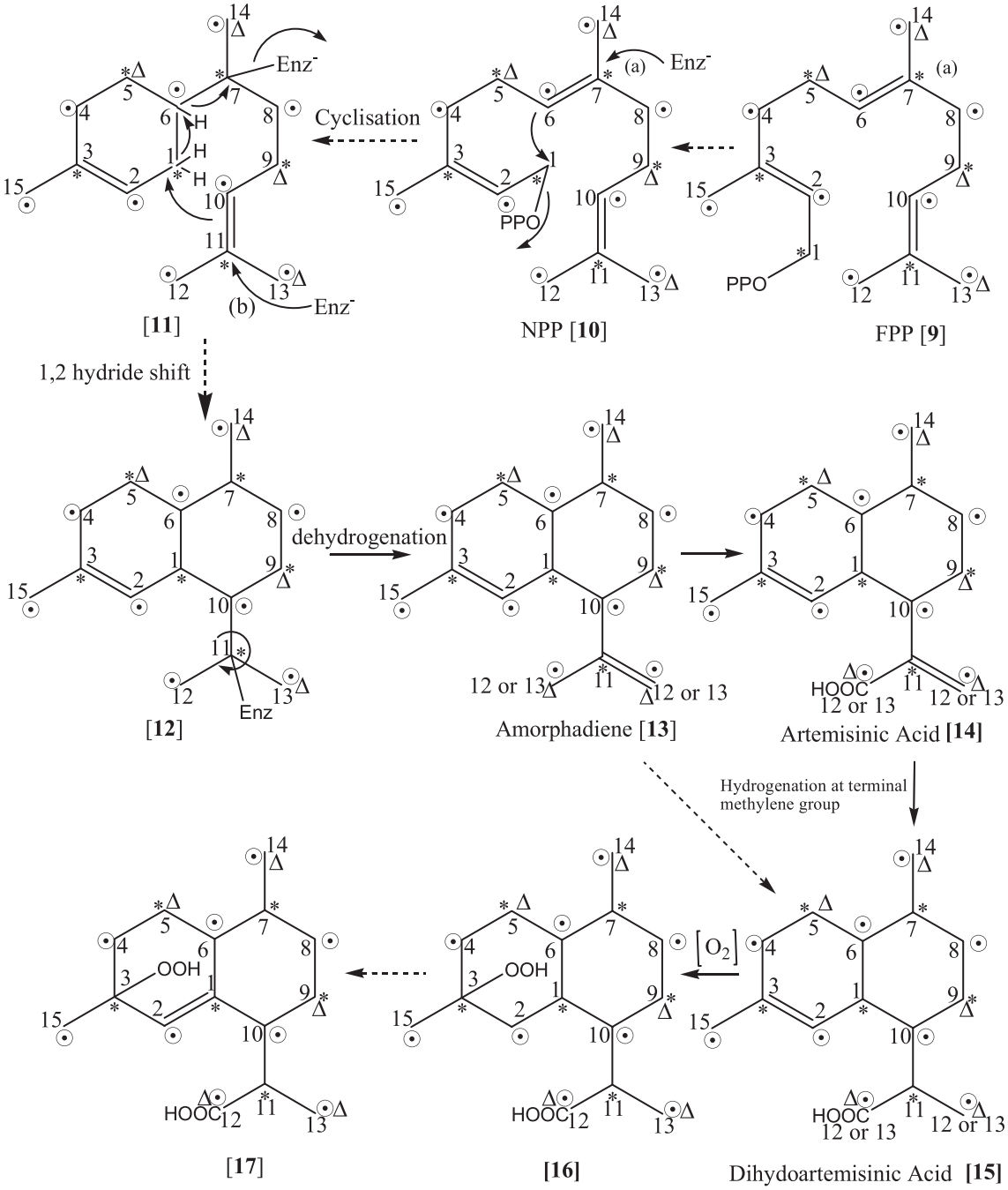

Figure 2. Proposed biosynthetic pathway from NPP (**9**) to allylic hydroperoxide (**17**) intermediate en *route* to artemisinin (**21**). Broken arrows indicate the presence of hypothetical pathway involving free or enzyme bonded intermediates which were difficult to isolate.

^{13}C-signals of six carbons (C-1, C-3, C-5, C-7, C-9, and C-11), whereas ^{13}C-enriched artemisinin obtained from [2-^{13}C]acetate showed enrichments at nine carbon atoms (C-2, C-4, C-6, C-8, C-10, C-12, C-13, C-14, and C-15) (Figure 4, Table 1). These findings could be explained through the schematic representation shown in Figures 1–3. The IPP (**6**) and DMAPP (**7**) units combine to form GPP (**8**) which combines with another molecule of IPP to form (*E*,*E*)-FPP (**9**) (Schramek et al. 2010). Because of the possible stereochemical requirements for cyclization to cadinane skeleton before the formation of amorphadiene (**13**) the (*E*,*E*)-FPP (**9**) may be converted to NPP (**10**), the (*E*,*Z*)-isomer of FPP (Picaud et al. 2005) (Figure 1), although this step has not been claimed by many scientists but appears to be logical as mentioned above (Picaud et al. 2005). Later on, the enzymatic attack of amorphadiene cyclases in several steps produce amorphadiene (**13**). The initial attack at C-7 by nucleophile (enzyme) possibly triggers the reaction, and a nucleophilic attack by $\Delta^{6,7}$ on C-1 of NPP (**10**) releases the pyrophosphate moiety to generate a possible unstable enzyme bond intermediate (**11**). In the process another enzymatic attack at C-11 induces $\Delta^{10,11}$ to attack the electron deficient site C-1 of **11** followed by hydrogen shift

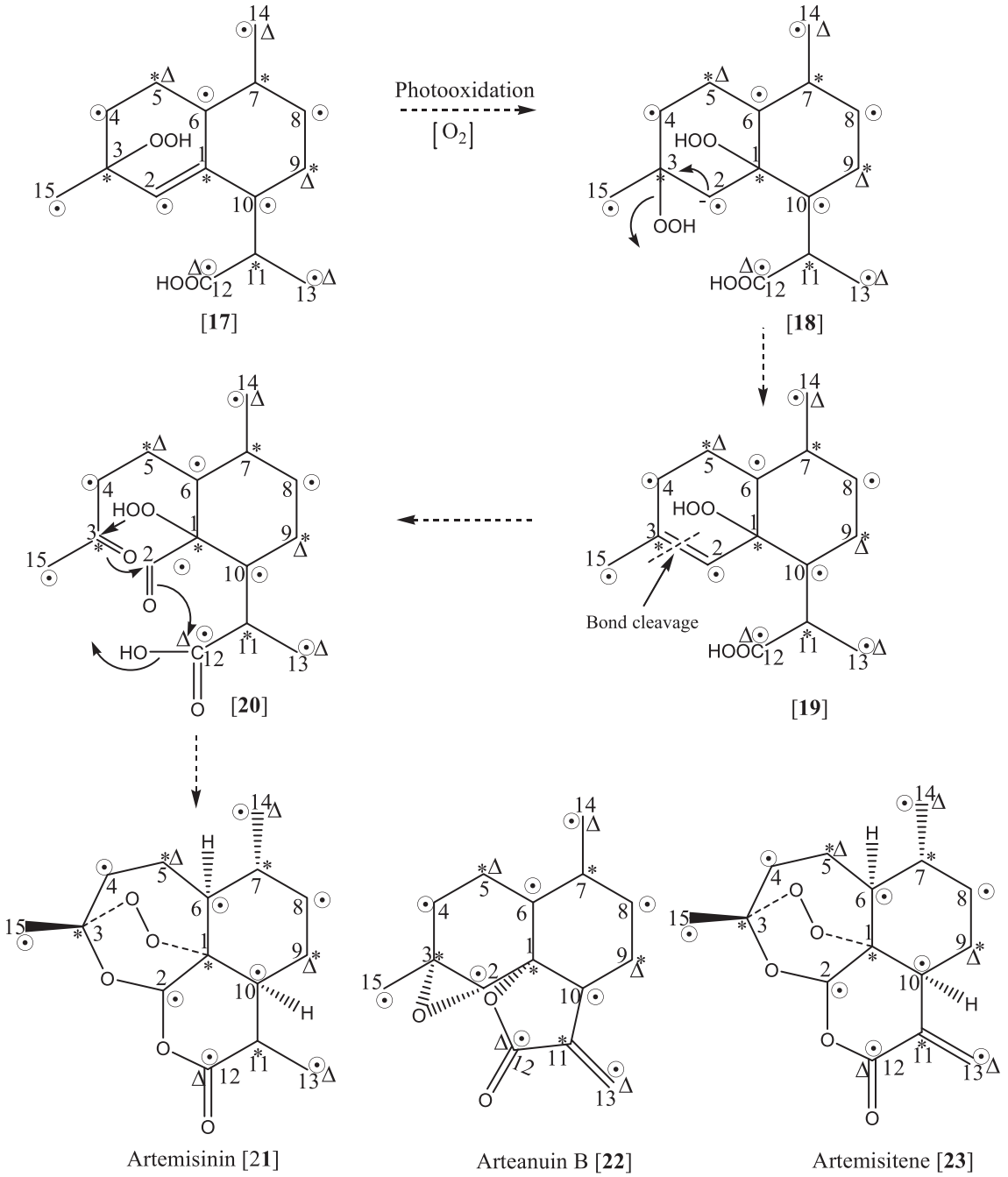

Figure 3. *, ⊙, denote label from [1-^{13}C]acetate and [2-^{13}C]acetate when biogenetic route to artemisinin (**21**) is achieved from IPP and DMAPP through MVA pathway; Δ denotes label from [1,6-$^{13}C_2$]glucose if GPP biosynthesized from IPP and DMAPP through DXP pathway plays and important role in the biosynthesis of **21**. Broken arrows indicate the presence of hypothetical pathway involving free or enzyme bonded intermediates which were difficult to isolate.

from C-1 to C-6 and another hydrogen shift from C-6 to C-7. This finally eliminates the attached enzyme from C-7 and possibly produces another unstable enzyme bond species (**12**). **12** is biogenetically an important intermediate because at this stage the C-10 and C-11 bond becomes free for rotation, and the identity of C-12 and C-13 methyl groups, initially obtained from DMAPP, is likely to be lost. The loss of originality of C-12 and C-13 is discussed further in the experiment done by feeding [1,6-$^{13}C_2$]glucose. In order to produce a terminal methylene group a hydrogen is lost either from C-12 or C-13 to produce amorphadiene (**13**). The terminal methyl (C-12 or C-13) of isopropyl group of **13** is oxidized through a chain of reactions involving CYP (P450 enzymes), aldehyde dehydrogenase (ALDH) to form artemisinic acid (**14**). Further, Dbr2 and artemsinic aldehyde $\Delta^{11,13}$ double bond reductase convert artemisinic aldehyde to dihydroartemisinic acid (**15**). Artemisinic acid (**14**) and dihydroartemisinic acid (**15**) (Figure 2) have been considered to be the potent precursors for artemisinin (**21**). Further, the peroxidation of C-2, C-3 double bond and internal rearrangements may produce the unstable intermediates **16** and **17**. The

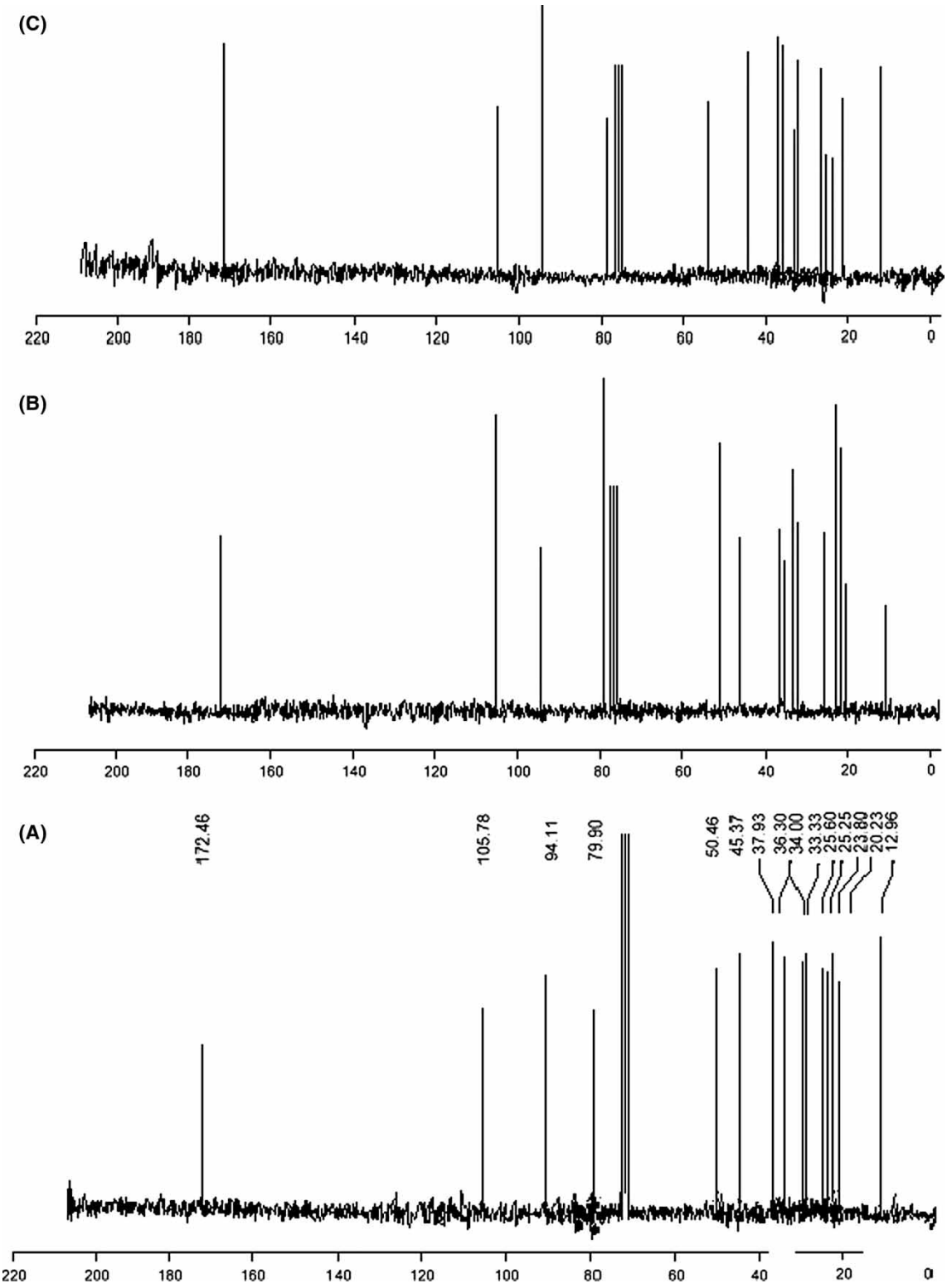

Figure 4. (a) ^{13}C-NMR of artemisinin isolated from *A. annua*. (b) ^{13}C-NMR of artemisinin isolated from *A. annua* after feeding [1-^{13}C]acetate. (c) ^{13}C-NMR of artemisinin isolated from *A. annua* after feeding [2-^{13}C]acetate. Enriched signals of ^{13}C are seen in (b) and (c).

biosynthetic steps shown with broken arrows indicate the presence of unstable intermediates which were difficult to isolate. The cleavage of $\Delta^{2,3}$ in **17** is initiated by peroxidation of $\Delta^{1,2}$ to yield another possible intermediate (**18**). It is believed that the final steps of biosynthesis of artemisinin (**21**) take place through a series of nucleophilic additions, elimination of peroxide, cleavage of $\Delta^{2,3}$, and elimination of hydroxyl group (Figure 3) [**17**→**18**→**19**→**20**→**21**]. The ^{13}C-peak enrichment of carbon atoms in artemisinin (**21**) support the MVA biogenetic pathway operating in the cytosol. Arteanuin B (**22**) and

Table 1. Incorporation of [1-^{13}C]acetate, [2-^{13}C]acetate, and [1,6-$^{13}C_2$]glucose into artemisinin (**1**) in *Artemisia annua*.

		Precursor fed					
		[1-^{13}C]acetate		[2-^{13}C]acetate		[1,6-$^{13}C_2$]glucose	
Artemisinin[a]		MVA pathway		MVA pathway		DXP pathway	
^{13}C-Chemical Shift assignment	δ (ppm)[b]	δ (ppm)[b]	Enrichment factor[c] (Relative enrichment)	δ (ppm)[b]	Enrichment factor[c] (Relative enrichment)	δ (ppm)[b]	Enrichment factor[c] (Relative enrichment)
C-1	79.90	79.91	**2.0**	79.92	0.1	79.91	0.2
C-2	94.11	94.12	0.2	94.11	**1.4**	94.12	0.3
C-3	105.78	105.79	**1.8**	105.73	0.3	105.77	0.3
C-4	36.30	36.29	0.2	36.27	**1.6**	36.28	0.3
C-5	23.80	23.80	**1.6**	23.81	0.2	23.80	**1.4**
C-6	37.92	37.89	0.3	33.90	**1.7**	33.93	0.4
C-7	34.00	33.96	**1.3**	33.96	0.3	33.97	0.2
C-8	33.33	33.33	0.4	33.32	**1.7**	33.33	0.3
C-9	25.25	25.25	**1.8**	25.23	0.0[d]	25.24	**1.6**
C-10	45.37	45.35	0.3	45.36	**1.8**	45.34	0.4
C-11	50.46	50.45	**1.9**	50.44	0.4	50.43	0.3
C-12	172.46	172.50	0.3	172.48	**1.8**	172.49	**1.5**
C-13	20.23	20.24	0.2	20.22	**1.5**	20.24	**1.4**
C-14	12.96	12.96	0.0[d]	12.94	**1.7**	12.95	**1.5**
C-15	25.60	25.60	0.4	25.58	**1.7**	25.61	0.2

Bold values indicate the 13C enriched peaks.
[a]Numbering pattern in artemisinin corresponds to that shown in Figure 3.
[b]$CDCl_3$ has been used as reference.
[c]Enrichment factor has been calculated by comparison of relative intensities of signals in the ^{13}C NMR spectra of ^{13}C-labeled **21** and a reference standard with ^{13}C at natural abundance. Enrichment factor = (Enriched integral – unlabelled integral)/unlabelled integral.
[d]Denotes the carbon used as reference to calculate the integration ratio.

artemisitene (**23**) are two biogenetically important compounds found in this plant. The biogenetic pathway to these compounds probably takes an individual route from artemisinic acid (**14**). If the $\Delta^{12,13}$ of **14** is not hydrogenated a similar path [**14**→**16**→**17**→**18**→**19**→**20**→**21**] will result into artemisitin (**23**) but this needs unequivocal confirmation. Similarly the epoxidation of $\Delta^{2,3}$ of artemisinic acid (**14**) and a lactone formation in-between C_1 and C_{12} may result in the formation of arteanuin B (**22**). We tried to isolate **22** and **23** from the same experiments along with artemisinin (**21**); however, the amounts of ^{13}C-enriched **22** and **23** were not substantial to run a ^{13}C-NMR spectra. The possible carbons to be enriched in **22** and **23** are shown in Figure 3. This may be proved in future studies and biosynthetic correlation between **21**, **22**, and **23** could be established.

The ^{13}C-NMR analysis of ^{13}C-enriched artemisinin (**21**) obtained from *A. annua* twigs which were fed with [1,6-$^{13}C_2$]glucose gave some interesting results (Table 1). As per documentation and earlier research the glucose metabolism to IPP (**6**) and DMAPP (**7**) takes place through DXP pathway which supposedly operates in plastids of the cell (Figure 1) and it can also get converted to acetate by the breakdown of pyruvate (Srivastava and Akhila 2010) and finally to IPP (**6**) and DMAPP (**7**) through MVA pathway. The tracer from [1,6-$^{13}C_2$]glucose is likely to achieve different positions in IPP (**6**) and DMAPP (**7**) through MVA and DXP pathways. It has been proved in many experiments that mono- and diterpenes are formed in the plastids by the combination of IPP (**6**) and DMAPP (**7**) units through DXP pathway. Artemisinin (**21**) is a sesquiterpene and unlikely to obtain any incorporation from ^{13}C-glucose through DXP pathway. However, artemisinin isolated from *A. annua* plants which were fed with [1,6-$^{13}C_2$]glucose showed enrichment at C-5, C-9, C-12, C-13, and C-14 (Table 1). Enrichment of these peaks can be explained through Figures 1–3. ^{13}C from C-1 and C-6 (**Δ**)of glucose attains position C-1 and C-5 in IPP and DMAPP (Figure 1), which may combine in the plastid itself in the presence of GPP synthase to make GPP (**8**). ^{13}C-enriched carbons (shown as **Δ**) in artemisinin (**21**, Figure 3) are the same for GPP which are enriched with ^{13}C as shown in Figure 1. The only exception being C-12 of artemisinin which is enriched with ^{13}C. This can be further explained that the GPP molecule travels through the plastidial membrane to cytosol where it combines with another IPP (**6**) which is already available there to form FPP (**9**) (Figure 1). Later on during the cyclization process, the gem-dimethyl groups lose their identity because of the free rotation along $\Delta^{10,11}$ and they become identical in nature. This results in the enrichment of ^{13}C-label as shown on C-12 and C-13. These findings are supported by earlier findings (Schramek et al. 2010) where GPP (**10**) has been shown to move from plastids to cytosol through an experiment which was conducted using

universal precursor $^{13}CO_2$ (Bacher and Eisenreich 2007).

Conclusions

The biosynthesis of artemisinin (**1**) has been reinvestigated using ^{13}C-labeled precursors, and the enrichment of carbon signals in ^{13}C-enriched artemisinin points out that MVA and DXP pathways participate in the biosynthetic process. MVA pathway is predominantly existent during the biosynthesis of **1** but it also involves geranyl (C_{10}) moiety biosynthesized in plastids via DXP pathway and once again proof of cross talk over between the plastid and cytosol constituents is indicated.

Acknowledgements

One of the authors (NS) is thankful to CSIR for Research Internship at CIMAP. Also, we are thankful to Director, CIMAP, for encouragement during the course of work. Our thanks are also due to Mr. M.R. Khan for helping us in maintaining the plants at CIMAP farm.

References

Akhila A, Rani K, Thakur RS. 1990. Biosynthesis of artemisinic acid in *Artemisia annua*. Phytochemistry. 29:2129–2132.

Akhila A, Thakur RS, Popli SP. 1987. Biosynthesis of artemisinin in *Artemisia annua*. Phytochemistry. 26:1927–1930.

Arigoni D, Sagner S, Latzel C, Eisenreich W, Bacher A, Zenk M. 1997. Terpenoid biosynthesis from 1-deoxy-D-xylulose in higher plants by intramolecular skeletal rearrangement. Proc Natl Acad Sci USA. 94:10600–10605 (and references cited therein).

Bacher A, Eisenreich W. 2007. ^{13}CO2 as a universal metabolic tracer in isotopologue perturbation experiments. Phytochemistry. 68:2273–2289.

Bertea CM, Voster A, Verstappen FWA, Maffei M, Beekwilder J, Bouwmeester HJ. 2006. Isoprenoid biosynthesis in *Artemisia annua*: cloning and heterologous expression of a germacrene A synthase from a glandular trichomes cDNA library. Arch Biochem Biophys. 448:3–12.

Bouwmeester HJ, Wallaart TE, Janssen MHA, Loo BV, Jansen BJM, Posthumus MA, Schmidt CO, Kraker JD, Kong WA, Franssen MCR. 1999. Amorpha-4,11-diene synthase catalyses the first probable step in artemisinin synthesis. Phytochemistry. 52:843–854.

Brown GD, Sy L. 2004. Synthesis of labeled dihydroartemisinic acid. Tetrahedron. 60:1125–1138.

Brown GD, Sy L. 2007a. In vivo transformation of artemisininc acid in *Artemisia annua* plants. Tetrahedron. 63:9548–9566.

Brown GD, Sy L. 2007b. In vivo transformation of dihydro-epi-deoxyarteannuin B in *Artemisia annua* plants. Tetrahedron. 63:9536–9547.

Covello PS, Teoh KH, Polichuk DR, Reed DW, Nowak G. 2007. Functional genomics and the biosynthesis of artemisinin. Phytochemistry. 68:1864–1871.

Delabays N, Simonnet X, Gaudin M. 2001. The genetics of artemisinin content in *Artemisia annua* L. and the breeding of yielding cultivars. Curr Med Chem. 8:1795–1801.

Eisenreich W, Rohdich F, Bacher A. 2001. Deoxyxylulose phosphate pathway to terpenoids. Trends Plant Sci. 6:78–84.

Eisenreich W, Sagner S, Zenk MH, Bacher A. 1997. Monoterpenoid essential oils are not of mevalonoid origin. Tetrahedron Lett. 38:3889–3892.

Eisenreich W, Schwarz M, Cartayrade A, Arigoni D, Zenk MH, Bacher A. 1998. The deoxyxylulose phosphate pathway of terpenoid biosynthesis in plants and microorganisms. Chem Biol. 5:221–233.

Ferreira JFS, Laughlin JC, Delabays N, Magalhaes PMD. 2005. Cultivation and genetics of *Artemisia annua* L. for increased production of the antimalarial artemisinin. Plant Gen Res. 3(2):206–229.

Hemmerlin A, Hoeffler J, Meyer O, Tritsch D, Kagan IA, Grosdemange-Billiard C, Rohmer M, Bach TJ. 2003. Crosstalk between the cytosolic mevalonate and the plastidial methylerythritol phosphate pathways in tobacco bright yellow-2 cells. J Biol Chem. 278:26666–26676.

Hoeffler J, Hammerlin A, Grosdemange-Billiard C, Bach TJ, Rohmer M. 2002. Isoprenoid biosynthesis in higher plants and in *Escherichia coli* on the branching in the methylerythritol phosphate pathway and the independent biosynthesis of isopentenyl diphosphate and dimethylallyl diphosphate. Biochem J. 366: 573–583.

Klayman DL. 1985. Qinghaosu (artemisinin): an antimalarial drug from China. Science. 228(4703):1049–1055.

Klayman DL, Lin AJ, Acton N, Scovill JP, Hock J, Milhous WK, Theoharides AD. 1984. Isolation of artemisinin (qinghaosu) from *Artemisia annua* growing in the United States. J Nat Prod. 47:715–717.

Lichtenthaler HK. 1999. The 1-deoxy-D-xylulose -5-phosphate pathway of isoprenoid biosynthesis in plants. Annu Rev Plant Physiol Plant Mol Biol. 50:47–65.

Lichtenthaler HK, Schwender J, Disch A, Rohmer M. 1997. Biosynthesis of isoprenoids in higher plant chloroplasts proceeds via a mevalonate independent pathway. FEBS Lett. 400:271–274.

Liu JM, Ni MY, Fan JF, Tu YY, Wu ZH, Wu YL, Chou WS. 1979. Structure and reaction of arteannuin. Acta Chim Sinica. 37:129–143.

Mercke P, Bengtsson M, Bouwmeester HJ, Posthumus MA. 2000. Molecular cloning, expression, and characterization of Amorpha-4,11-diene synthase, a key enzyme of artemisinin biosynthesis in *Artemisia annua* L. Arch Biochem Biophys. 381:173–180.

Olsson ME, Olofsson LM, Lindahl AL, Lundgren A, Brodelius M, Brodelius PE. 2009. Localization of enzymes of artemisinin biosynthesis to the apical cells of grandular secretory trichomes of *Artemisia annua* L. Phytochemistry. 70:1123–1128.

Picaud S, Mercke P, He X, Sterner O, Brodelius M, Cane DE, Brodelius PE. 2005. Amorpha-4,11-diene synthase: mechanism and stereochemistry of the enzymatic cyclisation of farnesyl diphosphate. Arch Biochem Biophys. 448:150–155.

Putalun W, Luealon W, Eknamkul WD, Tanaka H, Shoyama Y. 2007. Improvement of artemisinin

production by chitosan in hairy root cultures of *Artemisia annua* L. Biotechnol Lett. 29:1143–1146.

Rimada RS, Gatti WO, Jeandupeux R, Cafferata FR. 2009. Isolation characterization and qualification of artemisinin by NMR from Argentinean *Artemisia annua* L. Boletin Latinoamericano y del Caribe de Plantas Medicinales y Aromaticas. 8(4):275–281.

Ro D, Paradise EM, Ouellet M, Fisher KJ, Newman KL, Ndungu JM, Ho KA, Eachus RA, Ham TS, Chang MCY, et al.. 2006. Schematic representation of engineered artemisinic acid biosynthetic pathway in *S.cerevisiae* strain EPY224 expressing CYP71AV1 and CPR. Nature. 440:940–943.

Rohmer M. 1999. The discovery of a mevalonate-independent pathway for isoprenoid biosynthesis in bacteria, algae and higher plants. Nat Prod Rep. 16:565–574.

Rohmer M, Knani M, Simonin P, Sutter B, Sahm H. 1993. Isoprenoid biosynthesis in bacteria: a novel pathway for the early steps leading to isopentenyl diphosphate. Biochem J. 295:517–524.

Rohmer M, Seemann M, Horbach S, Bringer-Meyer S, Sahm H. 1996. Glyceraldehyde 3-phosphate and pyruvate as precursors of isoprenic units in an alternative non-mevalonate pathway for terpenoid biosynthesis. J Am Chem Soc. 118:2564–2566.

Schramek N, Wang H, Romisch-Margl W, Keil B, Radykewicz T, Winzenhorlein B, Beerhues L, Bacher A, Rohdich F. 2010. Artemisinin biosynthesis in growing plants of *Artemisia annua*. A 13CO2 study. Phytochemistry. 71:179–187.

Schuhr CA, Radykewicz T, Sagner S, Latzel C, Zenk MH, Arigoni D, Bacher A, Rohdich F, Eisenreich W. 2003. Quantitative assessment of crosstalk between the two isoprenoid biosynthesis pathways in plants by NMR spectroscopy. Phytochem Rev. 2:3–16.

Schwarz MK. 1994. Terpen-biosynthese in *Ginkgo biloba*: Eine Oberraschende Geschichte. [Terpene biosynthesis in *Ginkgo biloba*: a surprising story] Thesis Nr. 10951, Schweiz: ETH Zurich.

Srivastava N, Akhila A. 2010. Biosynthesis of andrographolide in *Andrographis paniculata*. Phytochemistry. 71:1298–1304.

Sy L, Brown GD. 2002. The mechanism of the spontaneous autoxidation of dihydroartemisinic acid. Tetrahedron. 58:897–908.

Towler MJ, Weathers PJ. 2007. Evidence of artemisinin production from IPP streaming from both the mevalonate and the nonmevalonate pathways. Plant Cell Rep. 26:2129–2136.

World Health Organization. 1981. Report of the fourth meeting of the scientific working group on the chemotherapy of malaria. Beijing, People's Republic of China, October 6–10. Geneva, Switzerland: Office of Publications World Health Organization.